EMBO reports

scientific report

De novo formation, fusion and fission of mammalian COPII-coated endoplasmic reticulum exit sites

David J. Stephens

University of Bristol, Bristol, UK

Transport between the endoplasmic reticulum (ER) and Golgi is mediated by the sequential action of the COPII and COPI coat complexes. COPII subunits are recruited to the ER membrane where they mediate the selection of cargo for transport to the Golgi, and also membrane deformation and vesicle formation. New ER exit sites can be generated by lateral growth and medial fission (in *Pythium* sp.) or by *de novo* formation (in *Pichia pastoris*) but it is not known how mammalian ER exit sites form. Here, time-lapse imaging of COPII-coated structures in live mammalian cells reveals that the number of ER export sites increases greatly during interphase by *de novo* formation. These results show the fusion of pre-existing ER export sites and the fission of larger structures. These three mechanisms of *de novo* formation, fusion and fission probably cooperate to regulate the size of these sites in mammalian cells.

EMBO reports **4**, 210–217 (2003)

doi:10.1038/sj.embor.embor736

INTRODUCTION

The first membrane-traffic step in the mammalian secretory pathway is the COPII-mediated budding of vesicles from the endoplasmic reticulum (ER) (Barlowe *et al.*, 1994; Barlowe, 2002). These vesicles then either fuse with a pre-existing transport carrier or fuse homotypically to form transport carriers (TCs) that traffic to the Golgi apparatus (Stephens & Pepperkok, 2001; Horstmann *et al.*, 2002). The COPII coat is a multi-protein complex that is recruited to the membrane following GDP/GTP exchange on the small GTPase Sar1 catalysed by the transmembrane protein Sec12. This results in the recruitment of the Sec23–Sec24 complex followed by the Sec13–Sec31 complex (Barlowe, 2002). The Sec23–Sec24 complex—more specifically Sec23—acts as a GTPase-activating protein for Sar1 (Yoshihisa *et al.*, 1993). Two isoforms of Sec23 are known to exist in humans, Sec23A and Sec23Bp, which are 80% identical in amino-acid sequence (Paccaud *et al.*, 1996). Together these proteins, which form the COPII coat, mediate cargo selection and membrane deformation to generate coated vesicles (Barlowe, 2002). COPII vesicles rapidly uncoat and fuse to form a nascent TC (also known as a vesicular–tubular cluster or VTC) that is transported in a microtubule-dependent manner to the Golgi apparatus (Klumperman, 2000). Previous work has shown that COPII proteins coat specific regions of the ER membrane, known as COPII-coated ER exit sites or transitional ER (Orci *et al.*, 1991; Hammond & Glick, 2000; Stephens *et al.*, 2000). Live cell imaging reveals that these sites are very stable, long-lived structures (Hammond & Glick, 2000; Stephens *et al.*, 2000) that direct the recycling of COPII components during successive rounds of cargo selection and vesicle budding. Furthermore, these sites are seen to increase in number during interphase before mitosis (Hammond & Glick, 2000; Prescott *et al.*, 2001).

Recently, considerable debate has focused on the mechanism by which the Golgi is inherited during mitosis (for review see Warren & Shorter, 2002). There are two principal mechanisms proposed for Golgi inheritance in mammalian cells. The first proposes that the Golgi fragments into a number of mitotic Golgi clusters (MGCs) that are partitioned between the two daughter cells (Warren & Shorter, 2002). These MGCs are frequently found in close proximity to ER exit sites (Lucocq *et al.*, 1989; Prescott *et al.*, 2001). Similarly, Golgi matrix structures are also located adjacent to, but distinct from, ER exit sites in mitosis (Lucocq *et al.*, 1989; Seemann *et al.*, 2002). The alternative hypothesis centres on the transfer of Golgi enzymes to the ER and the subsequent re-emergence through ER exit sites (Lippincott-Schwartz & Zaal, 2000). Considerable evidence therefore points to a role for ER exit sites in either of these possible mechanisms.

In the present study, a cell line stably expressing Sec23A coupled to yellow fluorescent protein (YFP) has been generated and analysed by long-term time-lapse imaging to investigate the dynamics of ER cargo export sites in mammalian cells. Significantly, these data show for the first time that COPII-coated ER exit sites are generated *de novo* in mammalian cells. In addition, these sites undergo fusion and fission events at approximately equal frequency. Furthermore, new ER export sites are functional in transport from the ER to the Golgi and accumulate in the juxtanuclear area of the cell after a slow translocation from the periphery. The large increase in the number of ER exit sites is correlated with the appearance of these sites and associated Golgi matrix and membranes at a position adjacent to, but separate from, the interphase Golgi stack. These results are consistent with models of self-organization to generate and maintain ER exit sites.

Department of Biochemistry, University of Bristol, School of Medical Sciences, University Walk, Bristol BS8 1TD, UK
Tel: +44 117 928 9955; Fax: +44 117 928 8274;
E-mail: david.stephens@bristol.ac.uk

Received 10 October 2002; revised 14 November 2002; accepted 3 December 2002

RESULTS

YFP–Sec23A as a marker of COPII function

Previous work has used fluorescent-protein-tagged versions of both Sec24D (Stephens *et al.*, 2000) and Sec13 (Hammond & Glick, 2000) in studies of COPII dynamics in living cells. The generation of a stable HeLa cell line expressing YFP–tagged Sec23A has enabled us to perform much longer-term imaging of COPII structures in cells than had previously been possible by transient expression (Stephens *et al.*, 2000). YFP–Sec23A localizes to a punctate distribution in these cells (Figure 1) identical to that seen with green fluorescent protein (GFP)-tagged Sec24D (Stephens *et al.*, 2000). YFP–Sec23A was characterized in both transient and stably expressing HeLa cells and shown to be a faithful marker of COPII function in living cells by the following criteria: when expressed in either HeLa or Vero cells, YFP–Sec23A co-localizes with Sec24, Sec13 and Sec31; it does not inhibit transport when expressed at low level and interacts functionally with Sar1 *in vitro* and *in vivo* (data not shown). Furthermore, the dynamics of ER exit sites by rapid imaging (60 frames per minute), are identical to those of GFP–Sec24D (Stephens *et al.*, 2000) and entirely consistent with those of GFP–Sec13 (Hammond & Glick, 2000). Imaging protocols used here were not found to inhibit progression or completion of the cell cycle (data not shown).

ER export sites increase in number during interphase

HeLa cells expressing YFP–Sec23A were imaged for many hours at a data acquisition rate of 1 frame per minute (Fig. 1 and Supplementary Information). In analysis of these experiments, structures in the cell periphery were specifically selected for analysis to permit the unequivocal identification of individual COPII structures. All images were acquired by wide-field microscopy. YFP–Sec23A HeLa cells are morphologically quite flat, which permits imaging of the entire depth of the cell in the periphery. Analysis of these data showed that during interphase of the cell cycle the number of ER export sites increases markedly (seen clearly in Fig. 1B, which shows enlarged images of the same cell as in Fig. 1A). Comparison of time points separated by 4 h showed that the number of peripheral sites increases by ~50% over this time (Fig. 1B). Analysis of small areas (~100 μm^2) of peripheral cytoplasm from eight cells showed that the number of sites increased by an average of 55 ± 8% (s.e.m.) over a 4-h period.

Interestingly, analysis of the time-lapse data from these experiments (see Supplementary Information) reveals that the newly formed peripheral ER export sites slowly translocate to the juxtanuclear area of the cell. This movement occurs with a net displacement towards the juxtanuclear area (as defined by the region of most intense

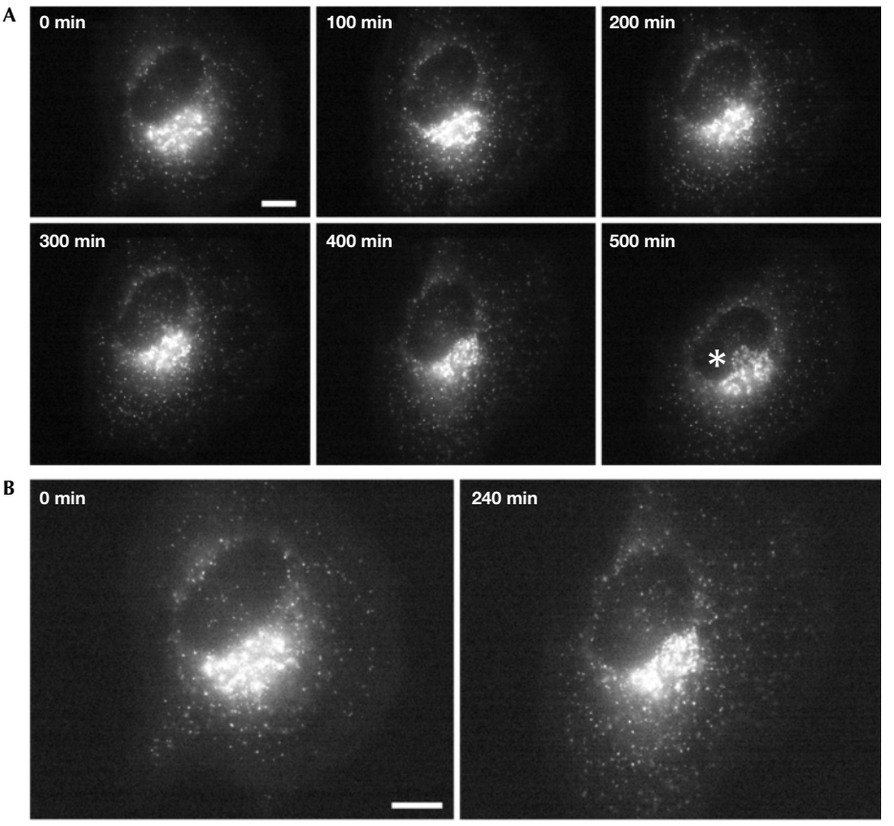

Fig. 1 | COPII-coated ER export sites greatly increase in number through interphase. Live cell imaging of YFP–Sec23A during interphase shows a marked increase in the number of COPII-coated ER exit sites. (**A**) Numbered frames correspond to minutes after the start of imaging. Images were acquired at 1 min intervals. The asterisk at 500 min of imaging denotes the migration of fluorescent structures from the juxtanuclear area to a region above the nucleus. (**B**) Enlarged view of the same cells as in (**A**) at the start and after 240 min of imaging. Scale bar, 5 μm. See Supplementary Information, which clearly shows the translocation of these structures to the juxtanuclear area at a very low rate (~5–15 μm h^{-1}).

fluorescence) of 5–15 μm h^{-1} and is therefore not consistent with the rapid rate of ER-to-Golgi cargo transport (0.5–1 μm s^{-1}; see, for example, Stephens *et al.*, 2000). This movement was quantified as the linear displacement of particles from their start point over 1 h; note that this is not a reflection of the *total* distance moved by these particles during this relocation, because movement is not linear or continuous.

Intriguingly, the translocation of COPII structures to the centre of the cell is correlated with the relocation of a subset of sites and of associated Golgi membranes to a localization above the nucleus (as seen by the accumulation of COPII (YFP–Sec23A) in this area, marked with an asterisk in Fig. 1). The location of this accumulation of structures above the nucleus is apparent from Z-sections of cells using both confocal and wide-field microscopy (not shown). This reorganization seems to occur consistently towards the end of interphase (seen before cells enter mitosis and in cells in which chromatin condensation and nuclear envelope breakdown are seen; data not shown). Figure 2 shows that the accumulation of Sec23A-positive structures above the nucleus (Fig. 2A–H, arrows;

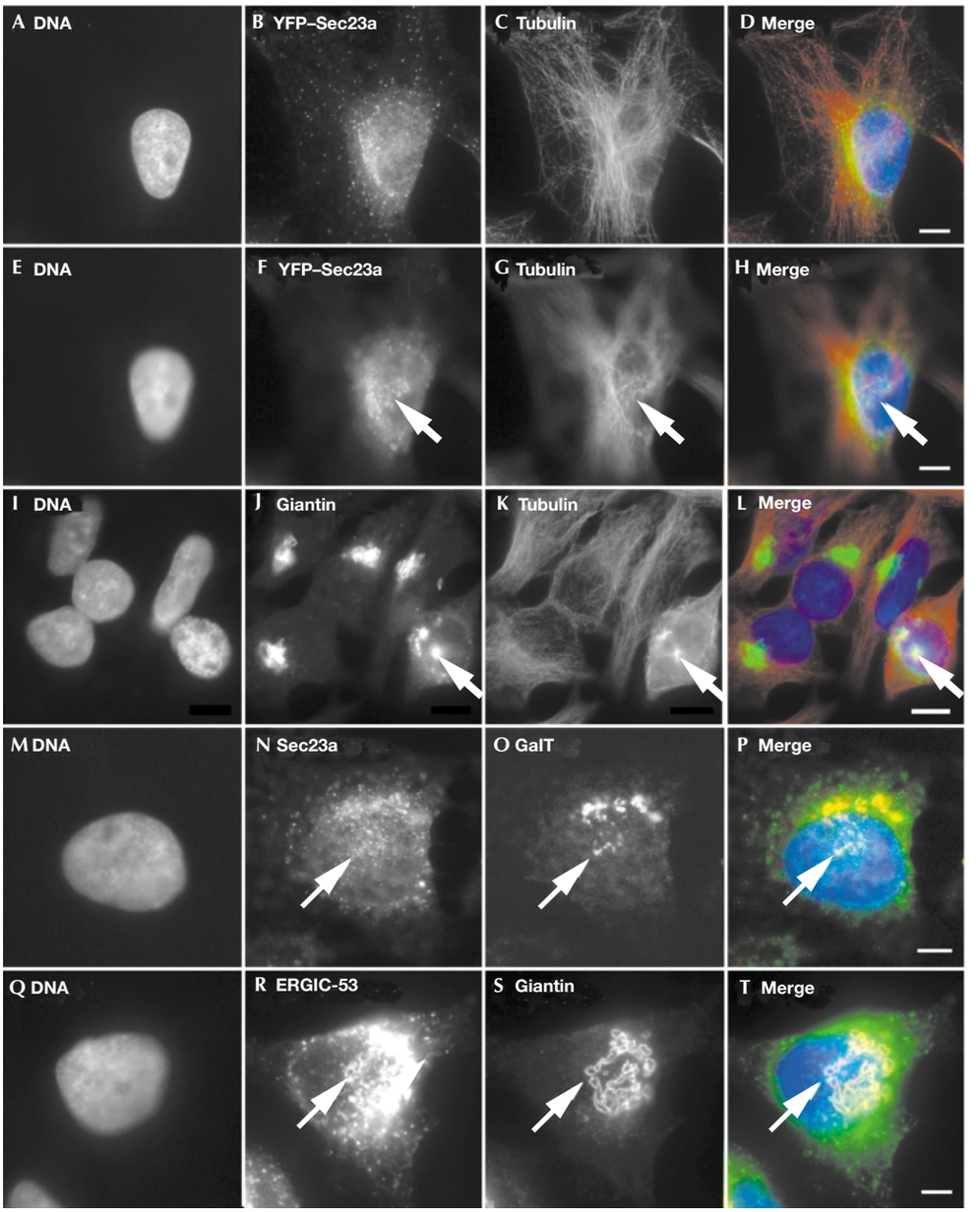

Fig. 2 | Relocation of YFP–Sec23A to an area above the nucleus is correlated with changes in the microtubule network and is accompanied by a relocation of Golgi matrix and membranes. (**A–C, E–G**) Images of the same cell at different focal planes, showing DNA, YFP–Sec23A and tubulin, as indicated. (**I–K**) DNA with giantin and tubulin immunofluorescence; (**M–O**) DNA, Sec23A and galactosyltransferase (GalT) immunofluorescence; (**Q–S**) DNA, ERGIC-53 and giantin immunofluorescence, as indicated. (**D, H, L, P, T**) Merged images of the preceding three panels in each case. Scale bars, 5 μm except for (**I–L**), where scale bar represents 15 μm.

note that the images in Fig. 2E–H have been intentionally focused on the area lying above the nucleus (arrow)) is correlated with a relocation of ERGIC-53-containing membranes (Fig. 2Q–T, arrows), a subset of Golgi matrix components (marked by giantin; Fig. 2I–L and Q–T, arrows) and membranes (marked by galactosyltransferase; Fig. 2M–P, arrows) to this area.

De novo formation of COPII-coated ER export sites

More detailed analysis of these time-lapse sequences revealed new fluorescent structures appearing in regions previously devoid of fluorescence (Fig. 3A; arrows denote pre-existing structures; arrowhead marks a newly appearing structure; panels represent 1 min intervals of imaging). Quantitative analysis of the fluorescent intensity of such structures reveals a progressive increase in intensity that rapidly (within 4 min) reaches a steady state similar to surrounding structures (Fig. 3B and C). Note that the intensities of the two original structures (Fig. 3B) are essentially unchanged after the formation of the third structure (Fig. 3C). These sites are clearly identifiable as forming *de novo* and often appear at locations some distance from other ER exit sites. Imaging of these cells over a period of up to 24 h showed that this process occurred throughout interphase.

COPII-coated sites undergo fusion and fission events

In addition to the *de novo* formation of COPII sites in the cytoplasm of these cells, fusion and fission events were also observed consistently. Figure 3D shows the fission of a single structure, resulting in the formation of two new structures. Interestingly, the fluorescence intensity of each of these two new structures (Fig. 3F) is more than half the intensity of the originating structure (Fig. 3E), suggesting the immediate recruitment of new material to these sites. Apparent fission is also observed in Fig. 3A–C (asterisk). It remains possible that fission events are in fact the separation of two independent exit sites, or the *de novo* formation of one site in direct proximity to another; light microscopy does not provide the axial resolution required to eliminate this possibility.

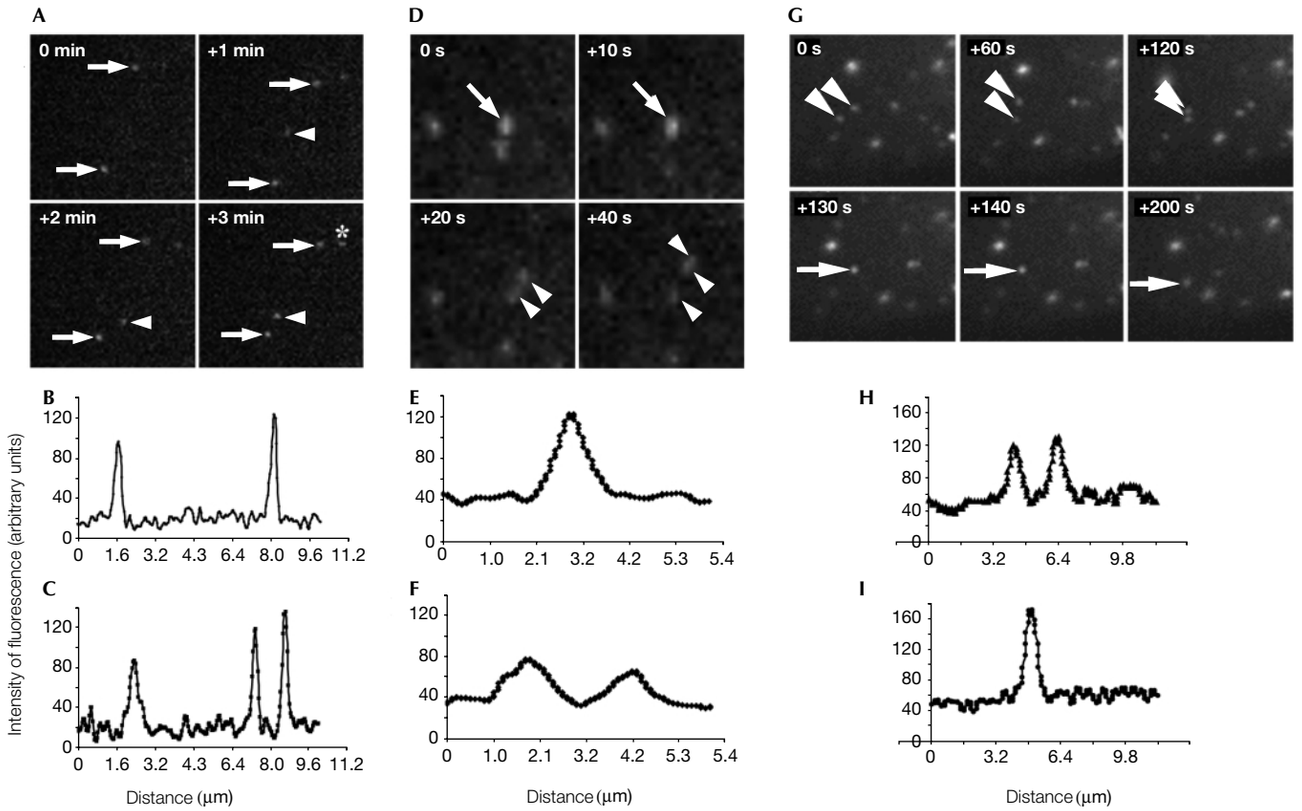

Fig. 3 | *De novo* formation, fission and fusion of COPII-coated ER export sites. (**A–C**) *De novo* formation of COPII-coated ER exit sites. (**A**) Frames are each separated by 1 min. Arrows highlight pre-existing structures; the arrowhead marks a newly appearing structure (appearing at +1 min). The asterisk marks a structure that seems to divide in the last minute of imaging (compare +1 min with +2 min). The dimensions of the region shown are 10.7 μm × 10.7 μm. (**B**, **C**) Plots of fluorescence intensity along a line drawn through and connecting the structures marked with arrows in (**A**), 0 min and +3 min respectively. (**D–F**) Fission of COPII-coated ER exit sites. A single, bright exit site (arrow) is seen to generate two discrete sites (+20 s); a further new site is seen adjacent to one of these (+40 s). The dimensions of the region shown are 8.1 μm × 8.1 μm. (**E**, **F**) Plots of fluorescence intensity across a diagonal line (passing through the single structure in (**D**), 0 s, and both structures in (**D**), +40 s). (**G–I**) Fusion of COPII-coated ER exit sites. Two COPII-coated structures are shown (arrowheads, 0–120 s) that undergo fusion and persist as a single structure (arrow, 130–200 s). The dimensions of the region shown are 11.4 μm × 11.4 μm. (**H**, **I**) Intensity profiles through the structures highlighted in (**G**), 0 s, and (**G**), 130 s, showing that the two structures seen at $t = 0$ s fuse to form one.

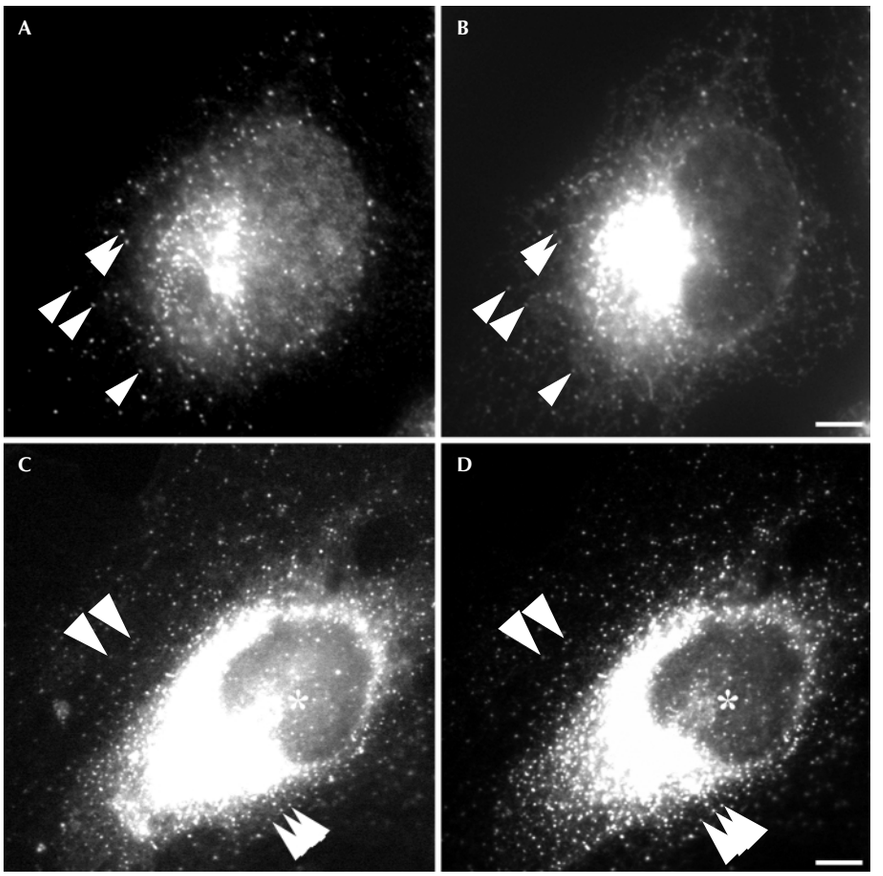

Fig. 4 | New ER export sites are functional in ER-to-Golgi transport. YFP–Sec23A-coated ER export sites co-localize with ERGIC-53 throughout interphase. (**A**, **B**) Early interphase; (**C**, **D**) late interphase (note the increased number of exit sites compared with (**A**) and (**B**), and the location of ER exit sites above the nucleus (asterisk)). (**A**, **C**) YFP–Sec23A; (**B**, **D**) anti-ERGIC-53 immunofluorescence. Arrowheads mark a selection of co-localizing structures. Scale bars, 5 μm.

Fusion of structures is also observed (Fig. 3G). Fusion was defined as having occurred once a single structure, formed from the merging of two structures, could be followed continuously for at least 10 min afterwards. After a fusion event, the fluorescence intensity of the resulting single structure was always less than double that of the intensity of the two original structures (Fig. 3H and I). From an analysis of small areas of cytoplasm, biased towards the cell periphery to simplify the classification of events, *de novo* formation was observed with a frequency of two events per hour per 100 μm^2; fusion and fission events were more frequent, each occurring four times per hour per 100 μm^2. Note that these figures exclude the large number of exit sites clustered in the juxtanuclear area and therefore specifically refer to peripheral exit sites.

ER exit sites forming *de novo* are functional

ER exit sites accumulate cargo adjacent to them in TCs; these TCs can be identified by the accumulation of ERGIC-53, an itinerant recycling cargo molecule. Immunofluorescence analysis of fixed cells expressing YFP–Sec23A with a monoclonal antibody against ERGIC-53 showed that 95–100% of YFP–Sec23A structures in any cell are positive for an ERGIC-53-containing TC and that this was independent of the number of ER export sites per cell (Fig. 4, compare panels A and B (early interphase) with panels C and D (late interphase); note the relocation of YFP–Sec23A and ERGIC-53 to a region above the nucleus (asterisk)). These ERGIC-53-containing TCs either superimpose directly or lie adjacent to ER exit sites, which is consistent with newly forming TCs. Results were identical for fixed cells and live cells that were imaged continuously for 4–8 h followed by fixation and immunostaining to permit the amplification of ER export sites during interphase. These results were also confirmed by immunostaining of non-transfected HeLa cells with antibodies directed against Sec23A and ERGIC-53 (data not shown).

YFP–Sec23A is predominantly cytosolic during mitosis

In accordance with previously published results, as cells enter metaphase, a redistribution of YFP–Sec23A to a diffuse localization is seen (Fig. 5). Comparison of fixation and immunostaining of non-transfected cells with live cell imaging of YFP–Sec23A-expressing cells reveals that punctate structures are seen during all stages of mitosis by immunofluorescence (Fig. 5A–T) but are not evident at metaphase by live cell imaging (Fig. 5U and V). This was confirmed by confocal microscopy (data not shown). This suggests that the YFP–Sec23A punctate structures seen by immunofluorescence might be an artefact of fixation or that remaining exit sites that have previously been

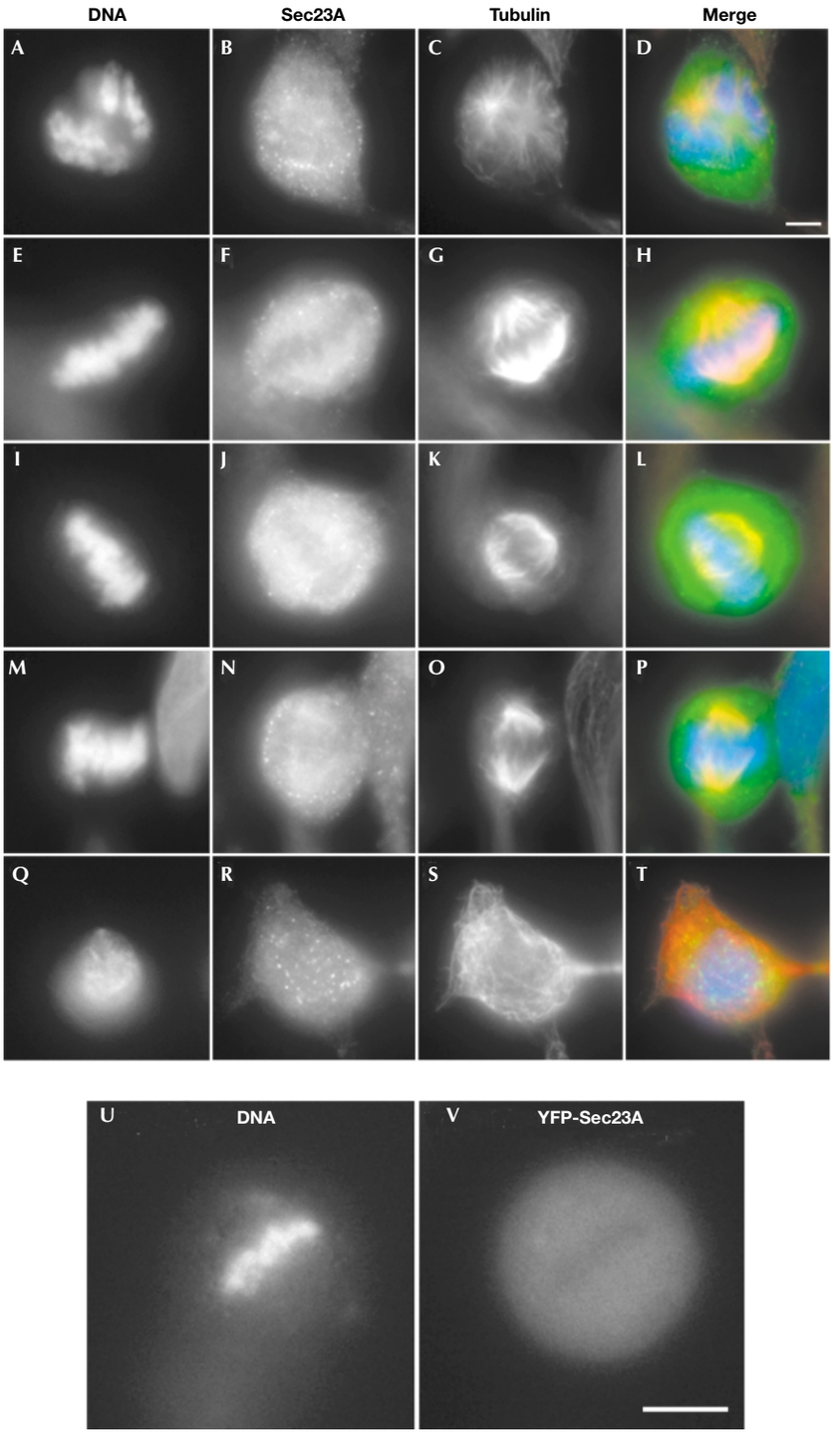

Fig. 5 | YFP–Sec23A is transiently redistributed to the cytosol during mitosis. Distribution of Sec23A during mitosis: prophase/prometaphase (**A–D**); metaphase (**E–H**); metaphase (**I–L**); early anaphase (**M–P**); telophase (**Q–T**) (note midbody stained with α-tubulin linking to that adjoining daughter cell). (**U**, **V**) Imaging of a living cell at mitosis reveals cytosolic localization of YFP–Sec23A during metaphase. (**A**, **E**, **I**, **M**, **Q**) DAPI staining; (**B**, **F**, **J**, **N**, **R**) Sec23A immunostaining; (**C**, **G**, **K**, **O**, **S**) α-tubulin staining; (**D**, **H**, **L**, **P**, **T**) merged images of the three preceding panels in each case. (**U**) DAPI image showing chromosomes aligned at metaphase; (**V**) YFP–Sec23A fluorescence showing diffuse labelling throughout the cell. Note that punctate Sec23A staining is seen throughout mitosis but the predominant localization is cytosolic, especially when chromosomes are aligned at metaphase. Scale bars, 5 μm.

characterized by electron microscopy (Prescott *et al.*, 2001) might be too small to be visualized because of the fluorescence resulting from the diffuse pool of YFP–Sec23A. It is also possible that the expression of YFP–Sec23A leads to destabilization of these sites during mitosis.

DISCUSSION

Previous results have shown that ER exit sites can be generated by one of two mechanisms: lateral growth and division of pre-existing sites, as seen in *Pythium* sp. (Bracker *et al.*, 1996), or *de novo* formation, as seen in *Pichia pastoris* (Bevis *et al.*, 2002). In both of these organisms, formation of new ER exit sites is inherently linked with the division of the Golgi in mitosis. Here, imaging of living mammalian cells expressing a component of the COPII complex has permitted the characterization of the dynamics of COPII-coated ER exit sites (with exit sites defined by the association of COPII proteins; see Stephens *et al.*, 2000). From these experiments, I have shown that fusion and fission of existing sites, as well as *de novo* formation of new sites, all occur in mammalian cells. These data are in agreement with recently published work characterizing the dynamics of these sites in *P. pastoris* (Bevis *et al.*, 2002).

These results are also consistent with a proposed model for self-organization of ER export sites, in which the controlled size of these sites results from a balance between the budding of COPII vesicles and the recruitment of new molecules at the edge of these sites (Bevis *et al.*, 2002). Although fusion and fission events would result in gross control over size of these structures, the observation that exit sites formed *de novo* and those formed by apparent fission both rapidly recruit more YFP–Sec23A suggests an additional fine control over size. Qualitative examination of many independent experiments shows that it is brighter structures that are more likely to undergo fission events, whereas dimmer structures are more likely to fuse to form brighter (and by inference larger) structures. The ability to regulate the number of ER exit sites would provide an adaptive mechanism for the temporal regulation of secretory requirements. Indeed, previous work has shown a correlation between cargo and ER exit site number (Aridor *et al.*, 1999) and is consistent with *de novo* formation of ER exit sites possibly triggered by cargo molecules themselves. In addition, the amplification of the number of ER export sites throughout interphase and inheritance of the ER by stochastic processes during mitosis (Zeligs & Wollman, 1979) would ensure an appropriate segregation of export sites between daughter cells.

Fusion and fission events occur more frequently than *de novo* formation events, suggesting that a further slight increase in the frequency of fission would provide a rapid means for an adaptive increase in the number of exit sites. However, these analyses overestimate the number of fission events and underestimate the number of *de novo* formation events because one cannot discriminate between genuine fission events and *de novo* formation of sites in direct proximity to a pre-existing site. This leads to the conclusion that *de novo* formation is likely to be the principal mechanism for the generation of new peripheral ER exit sites in mammalian cells. From these data, one cannot exclude the possibility that both mechanisms are responsible for the increase in number of exit sites.

An interesting observation from the data is the slow migration of ER exit sites from the periphery towards the juxtanuclear area of the cell over time. The timescale of this movement means that this is unlikely to reflect the presence of COPII-coated transport carriers; indeed, COPII is not seen to coat TCs moving towards the Golgi (Stephens *et al.*, 2000). Movement of ER exit sites towards the juxtanuclear region might reflect a functional coupling to (and subsequent transport along) microtubules or it might be an indirect effect of ER membrane remodelling in the cell periphery.

Importantly, there seem to be no functional differences between newly generated ER export sites and pre-existing ones: 95–100% of sites in cells are located adjacent to an ERGIC-53-positive structure that is assumed to be a newly forming TC (see Stephens *et al.*, 2000; Stephens & Pepperkok, 2002). Despite a marked increase in the number of exit sites during progression through interphase, there seems to be no discrimination with regard to the presence of TCs adjacent to these sites. It has not been possible to examine this in living cells owing to technical limitations of live cell imaging with tagged ERGIC-53; this is consistent with previous observations of the expression of recombinant ERGIC-53 (Schindler *et al.*, 1993).

A key question that remains is whether all components that go to make a mammalian ER exit site have been defined. Yeast and mammalian COPII systems are functionally equivalent to homologues of key components of the yeast COPII coat present in mammals (Barlowe, 2002). *De novo* formation of ER exit sites can proceed by self-organization mechanisms based on freely diffusible proteins within the ER membrane. Glick and colleagues (Bevis *et al.*, 2002) have proposed that Sec12 might have a role in coordinating the organization of ER exit sites in *P. pastoris*. Significantly, a mammalian homologue of Sec12 has recently been identified (Weissman *et al.*, 2001). A GFP-tagged form of the human homologue of Sec12 localizes throughout the ER, which is consistent with immunofluorescence localization of the endogenous protein (Weissman *et al.*, 2001), and shows free diffusion within the plane of the ER membrane (D.J.S, unpublished observations) and so would be capable of nucleating ER exit-site formation at new locations. An alternative explanation remains the templated assembly of COPII components onto a structural scaffold such as Sec16, a 250 kDa protein that is tightly but peripherally associated with the ER membrane in *Saccharomyces cerevisiae* (Barlowe, 2002). As yet there is no functional equivalent for Sec16 in mammalian cells.

METHODS

All chemical reagents were purchased from Sigma unless stated otherwise.

HeLa cells (ATCC number CCL-2) were grown in DMEM containing 10% fetal calf serum (Invitrogen). YFP–Sec23A was provided by Jean-Pierre Paccaud (Geneva, Switzerland). Cells were transfected with YFP–Sec23A and selected for stable expression with 0.5 mg ml^{-1} G418 (Invitrogen). Individual clones were amplified and visually screened for expression by fluorescence microscopy; clones were maintained in 0.25 mg ml^{-1} G418. In each case where a stable line was obtained it was found to be impossible to retain clonality; within 5–6 passages, 99% of cells had lost fluorescence while retaining resistance to the selection marker.

For immunofluorescence, cells were grown on 22 mm coverslips, fixed with methanol at –20 °C and immunostained as described (Stephens *et al.*, 2000). Antibodies used were as follows: anti-Sec23A rabbit polyclonal (Affinity Bioreagents), anti-ERGIC-53 mouse monoclonal (provided by Hans-Peter Hauri), anti-giantin rabbit polyclonal (Covance) and anti-tubulin mouse monoclonal (Neomarkers). Primary antibodies were detected by using anti-mouse or anti-rabbit secondary antibodies conjugated to Alexa-488, Alexa-568 or Alexa-647 (Cambridge Bioscience) and cells were counterstained with 4,6-diamidino-2-phenylindole (DAPI; Cambridge Bioscience). Living

and fixed cells were imaged with an Olympus/TILL Photonics imaging system comprising an Olympus IX-70 microscope with a PLAPO 100×, numerical aperture 1.40, oil-immersion objective (Olympus Optical Co.). Illumination was provided by a 150 W xenon lamp controlled by a Polychrome IV monochromator coupled to the microscope by a quartz light guide. Emission filters for cyan fluorescent protein/YFP and Cy5 were from Chroma. Images were captured with a TILL IMAGO SVGA camera controlled by TILL visION v.4.0 software and processed with Image J (http://rsb.info.nih.gov/ij) and Adobe Photoshop v.6.0 (Adobe Systems). Cells grown on live cell dishes (MatTek) were imaged at 37 °C with the microscope enclosed in a heated Perspex box (Solent Scientific) in MEM without phenol red, supplemented with 30 mM HEPES, pH 7.4, 0.5 g l^{-1} sodium bicarbonate and 10% fetal calf serum. Long-term imaging (up to 24 h) was achieved by completely filling dishes with medium and sealing the lid with high-viscosity vacuum grease.

Supplementary data are available at *EMBO reports* Online (http://www.emboreports.org).

ACKNOWLEDGEMENTS

I thank G. Banting, R. Pepperkok and H. Mellor for critical reading of the manuscript, and K. Palmer for technical assistance. I thank the Medical Research Council (UK) for providing an Infrastructure Award and Joint Research Equipment Initiative grant to establish the University of Bristol School of Medical Sciences Cell Imaging Facility. This work is supported by a Research Career Development Award (G120/617) from the Medical Research Council (UK).

REFERENCES

Aridor, M., Bannykh, S.I., Rowe, T. & Balch, W.E. (1999) Cargo can modulate COPII vesicle formation from the endoplasmic reticulum. *J. Biol. Chem.*, **274**, 4389–4399.

Barlowe, C. (2002) COPII-dependent transport from the endoplasmic reticulum. *Curr. Opin. Cell Biol.*, **14**, 417–422.

Barlowe, C. *et al*. (1994) COPII: a membrane coat formed by Sec proteins that drive vesicle budding from the endoplasmic reticulum. *Cell*, **77**, 895–907.

Bevis, B.J., Hammond, A.T., Reinke, C.A. & Glick, B.S. (2002) *De novo* formation of transitional ER sites and Golgi structures in *Pichia pastoris*. *Nature Cell Biol.*, **4**, 750–756.

Bracker, C.E., Morré, D.J. & Grove, S.N. (1996) Structure, differentiation and multiplication of the Golgi apparatus in fungal hyphae. *Protoplasma*, **194**, 250–274.

Hammond, A.T. & Glick, B.S. (2000) Dynamics of transitional endoplasmic reticulum sites in vertebrate cells. *Mol. Biol. Cell*, **11**, 3013–3030.

Horstmann, H., Ng, C.P., Tang, B.L. & Hong, W. (2002) Ultrastructural characterization of endoplasmic reticulum–Golgi transport containers (EGTC). *J. Cell Sci.*, **115**, 4263–4273.

Klumperman, J. (2000) Transport between ER and Golgi. *Curr. Opin. Cell Biol.*, **12**, 445–449.

Lippincott-Schwartz, J. & Zaal, K.J. (2000) Cell cycle maintenance and biogenesis of the Golgi complex. *Histochem. Cell Biol.*, **114**, 93–103.

Lucocq, J.M., Berger, E.G. & Warren, G. (1989) Mitotic Golgi fragments in HeLa cells and their role in the reassembly pathway. *J. Cell Biol.*, **109**, 463–474.

Orci, L. *et al*. (1991) Mammalian Sec23p homologue is restricted to the endoplasmic reticulum transitional cytoplasm. *Proc. Natl Acad. Sci. USA*, **88**, 8611–8615.

Paccaud, J.P. *et al*. (1996) Cloning and functional characterization of mammalian homologues of the COPII component Sec23. *Mol. Biol. Cell*, **7**, 1535–1546.

Prescott, A.R. *et al*. (2001) Evidence for prebudding arrest of ER export in animal cell mitosis and its role in generating Golgi partitioning intermediates. *Traffic*, **2**, 321–335.

Schindler, R., Itin, C., Zerial, M., Lottspeich, F. & Hauri, H.P. (1993) ERGIC-53, a membrane protein of the ER-Golgi intermediate compartment, carries an ER retention motif. *Eur. J. Cell Biol.*, **61**, 1–9.

Seemann, J., Pypaert, M., Taguchi, T., Malsam, J. & Warren, G. (2002) Partitioning of the matrix fraction of the Golgi apparatus during mitosis in animal cells. *Science*, **295**, 848–851.

Stephens, D.J. & Pepperkok, R. (2001) Illuminating the secretory pathway: when do we need vesicles? *J. Cell Sci.*, **114**, 1053–1059.

Stephens, D.J. & Pepperkok, R. (2002) Imaging of procollagen transport reveals COPI-dependent cargo sorting during ER-to-Golgi transport in mammalian cells. *J. Cell Sci.*, **115**, 1149–1160.

Stephens, D.J., Lin-Marq, N., Pagano, A., Pepperkok, R. & Paccaud, J.P. (2000) COPI-coated ER-to-Golgi transport complexes segregate from COPII in close proximity to ER exit sites. *J. Cell Sci.*, **113**, 2177–2185.

Warren, G. & Shorter, J. (2002) Golgi architecture and inheritance. *Annu. Rev. Cell Dev. Biol.*, **18**, 379–420.

Weissman, J.T., Plutner, H. & Balch, W.E. (2001) The mammalian guanine nucleotide exchange factor mSec12 is essential for activation of the Sar1 GTPase directing endoplasmic reticulum export. *Traffic*, **2**, 465–475.

Yoshihisa, T., Barlowe, C. & Schekman, R. (1993) Requirement for a GTPase-activating protein in vesicle budding from the endoplasmic reticulum. *Science*, **259**, 1466–1468.

Zeligs, J.D. & Wollman, S.H. (1979) Mitosis in rat thyroid epithelial cells in vivo. I. Ultrastructural changes in cytoplasmic organelles during the mitotic cycle. *J. Ultrastruct. Res.*, **66**, 53–77.